Advanced Features

1 Pyroelectric Detectors with JFET source follower or integrated CMOS-OpAmp – A Comparison

In 2003 InfraTec added pyroelectric detectors with integrated CMOS Operational Amplifiers (OpAmp) to our established family of detectors with integrated Junction Field Effect Transistors (JFET). Advancements in analog silicon based technologies have allowed us to replace the classic JFET design with a more complex amplification circuit for nearly all applications.

Well established JFET detector designs like the LME-302, LME-316 and LIM-222 have been enhanced with CMOS OpAmps as in the LME-351, LME-335 and LIM-262.

LME-316 with JFET (thermally compensated)   **LME-335 with CMOS OpAmp (thermally compensated)**

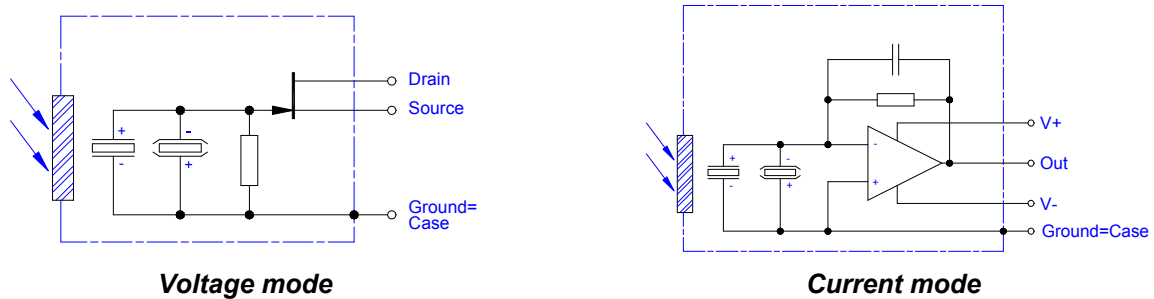*Voltage mode*   *Current mode*

Fig 1:   Examples of pyroelectric detectors with JFET (left side) and OpAmp (right side)

Detectors with JFET and OpAmp are distinguished by more than orders of magnitude in signal voltage. The fundamental difference you find is in the analysis of the pyroelectric signal. As a result you will get different frequency responses of signal and noise (response and typical parameters in figure 2).
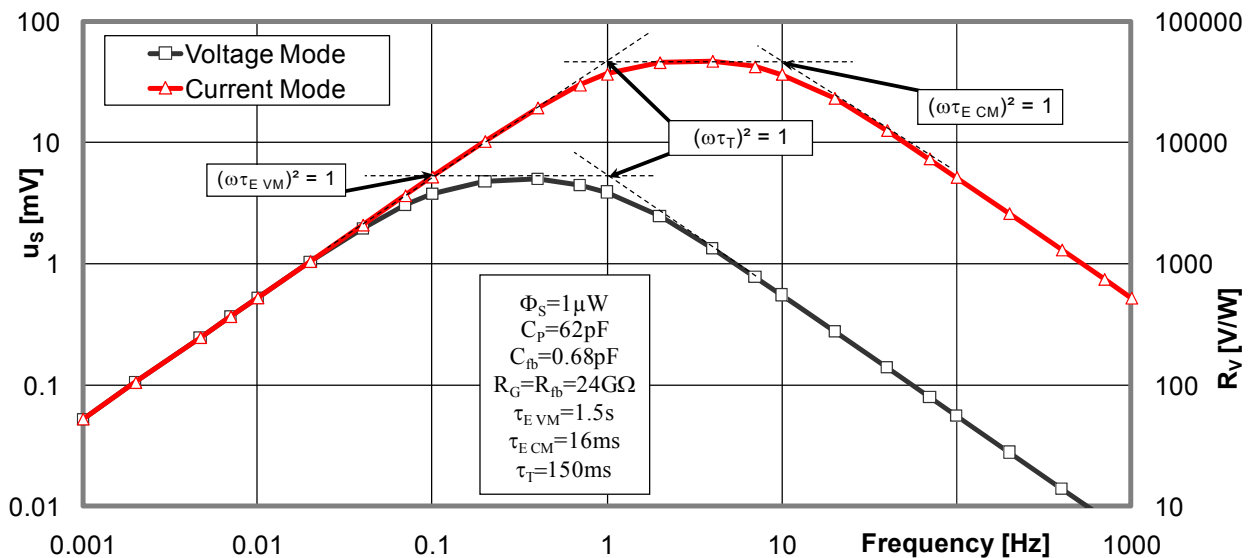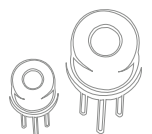

Fig 2:   Frequency response of signal voltage uS and voltage responsivity RV of a pyroelectric detector with (2 x 2) mm active sensing element

Advanced Features

In voltage mode the pyroelectric current, created in the single crystalline LiTaO$_3$ chip, charges the electric capacity. The resulting voltage is displayed by a simple source follower (JFET, gate resistor and external source resistor).

In current mode the generated pyroelectric current is transformed by a Current-Voltage-Converter (OpAmp with feedback components, also named Trans-Impedance-Amplifier TIA). The frequency dependent conversion factor I/U is determined by the complex feedback components and is typically in the range of (10 ... 200) pA/V. While the thermal time constant τ_T (typically 150 ms) as a measure of the thermal coupling of the pyroelectric element to its surrounding is effective in both operation modes, the electric time constant τ_E is determined by different components. In voltage mode τ_E is calculated as a product of pyroelectric chip capacity C_P and gate resistor R_G (typically 1.5 s). In current mode τ_E is only determined by the feedback components R_{fb} and C_{fb} (typically 16 ms).

Main differences between pyroelectric detectors with JFET and CMOS-OpAmp
- At common modulation frequencies between 1 Hz and 10 Hz in gas analysis and flame detection the detector will operate above the thermal and electrical time constant (1/f behavior of signal). The maximal responsivity is located beyond the normal modulation frequency range. Low-frequency disturbances up to some millihertz will be transmitted. Detectors need settling times up to some 10 seconds.
- Detectors in current mode are mostly operated between both time constants and resultant cut-on and cut-off frequency. Here the signal voltage is on its highest level and stable over a broad frequency range, possibly over some hundred Hertz. Low-frequency disturbances are one magnitude away from the cut-on frequency and will therefore by suppressed 10 times more compared to the voltage mode. The measuring signals are already stable after a few seconds.
- Due to the virtual short circuit of the pyroelectric element in current mode, an antiparallel connected compensation element does not lead to a reduction of signal and detectivity. Furthermore an incomplete illuminated pyroelectric element in current mode does not cause a loss of both signal and detectivity in contrast to the voltage mode.

Why we are using CMOS-Operational amplifiers?
CMOS technology combines technological and customer demands for a low supply voltage, low power consumption, Rail-to-Rail performance at output and low chip costs. Additionally, the completely isolating gate (SiO$_2$) in the operational amplifier shows a better performance during operation at high temperatures as opposed to the JFET design. The current mode, which earlier was only possible to apply in combination with very expensive OpAmps like OPA128 or AD549, can now be applied in applications for gas analysis and flame detection that were previously dominated both technologically and price wise by the JFET.

Comparison of the modulated output signal for detectors with JFET and OpAmp
The electrical time constant defines the form of the output signal in current and voltage mode. Identical time constants lead to the same signal form in both modes. In current mode we can work with a nearly arbitrary electrical time constant, which is an essential advantage. Therefore, short time constants are preferred due to the resulting short settling time.

InfraTec can assure the availability of detectors with JFET source follower and CMOS-OpAmp for many years to come. The technical advantages, however, will accelerate the trend to use the current mode OpAmp detectors.
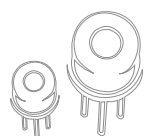
Advanced Features

Figures 3 to 6 show typical signal characteristics in order with decreasing electrical time constant.
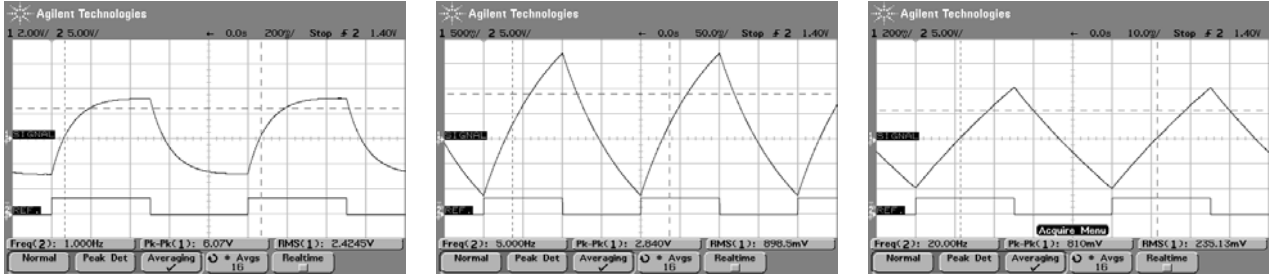

Fig 3:   LME-302 Voltage mode at 1 Hz, 5 Hz and 20 Hz, thermal time constant 150 ms, electrical time constant 5 s
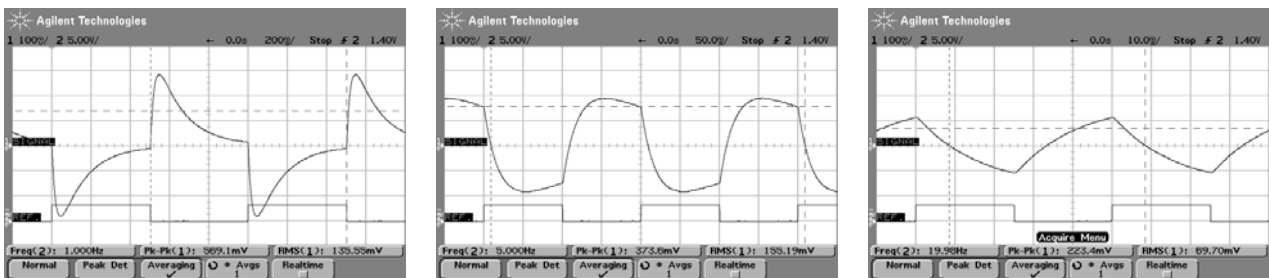

Fig 4:   LME-335 Current mode at 1Hz, 5 Hz and 20 Hz, thermal time constant 150 ms, electrical time constant 20 ms
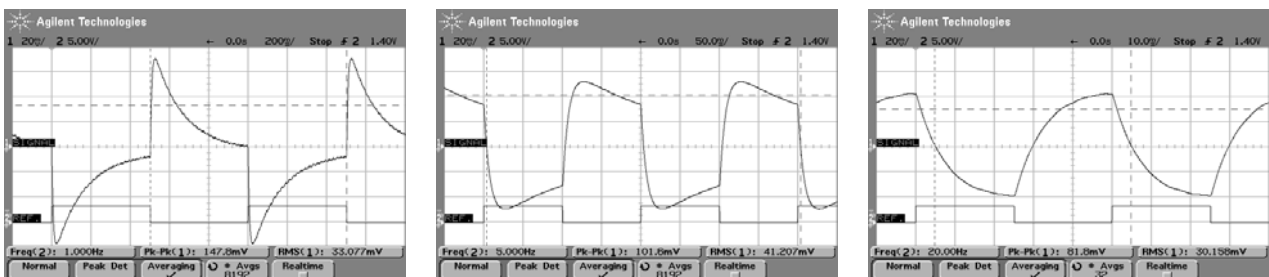

Fig 5:   LME-341 Current mode at 1 Hz, 5 Hz and 20 Hz, thermal time constant 150 ms, electrical time constant 5 ms
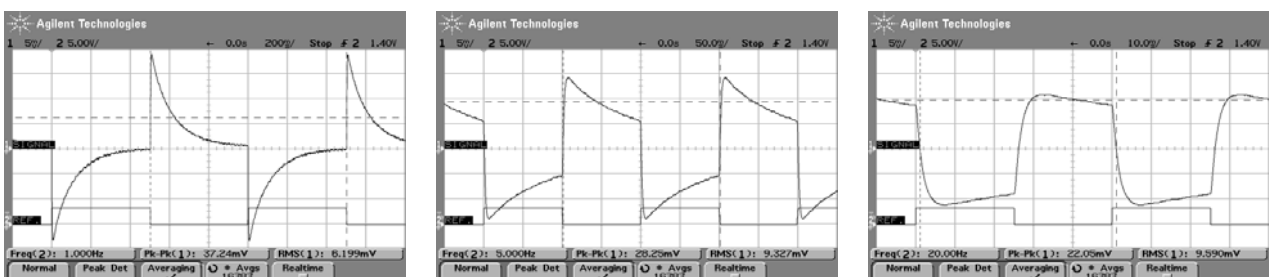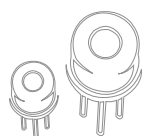

Fig 6:   LME-351 Current mode at 1 Hz, 5 Hz and 20 Hz, thermal time constant 150 ms, electrical time constant 1 ms

Advanced Features

The resistance rating of the integrated feedback or gate resistor leads to different detector properties.
For current mode detectors applies the following:

■ A large feedback resistor results in a high signal and an increased detectivity since the noise only increases with the square root of the resistor value. In contrast an amplifier stage after the detector would increase signal and noise by the same ratio.

■ A small resistor increases the stability of the DC operating point, therefore a thermal compensation is often not necessary for R<10 GOhm.
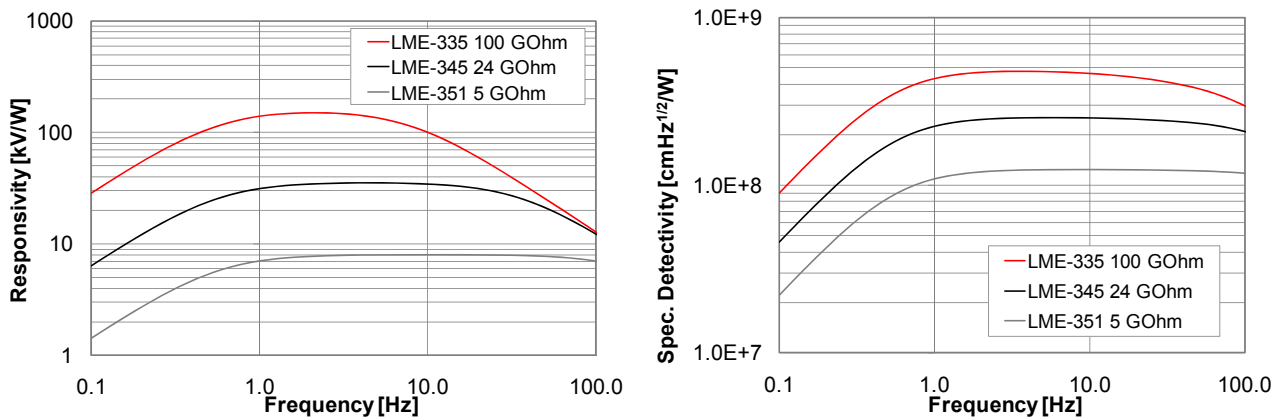
Fig 7: *Frequency response of responsivity (signal) and specific detectivity (signal-to-noise ratio) as a function of the feedback resistor in current mode detectors; LME-335 (100 GOhm), LME-345 (24 GOhm), LME-351 (5 GOhm)*

Voltage mode detectors behave as follows:

■ The gate resistor value is not determining the signal height for frequencies above the thermal corner frequency around 1 Hz. The noise is indirect proportional to the square root of the gate resistor value which results in a higher detectivity for detectors with a large gate resistor.

■ A small resistor increases the stability of the DC operating point, therefore a thermal compensation is often not necessary for R<10 GOhm.
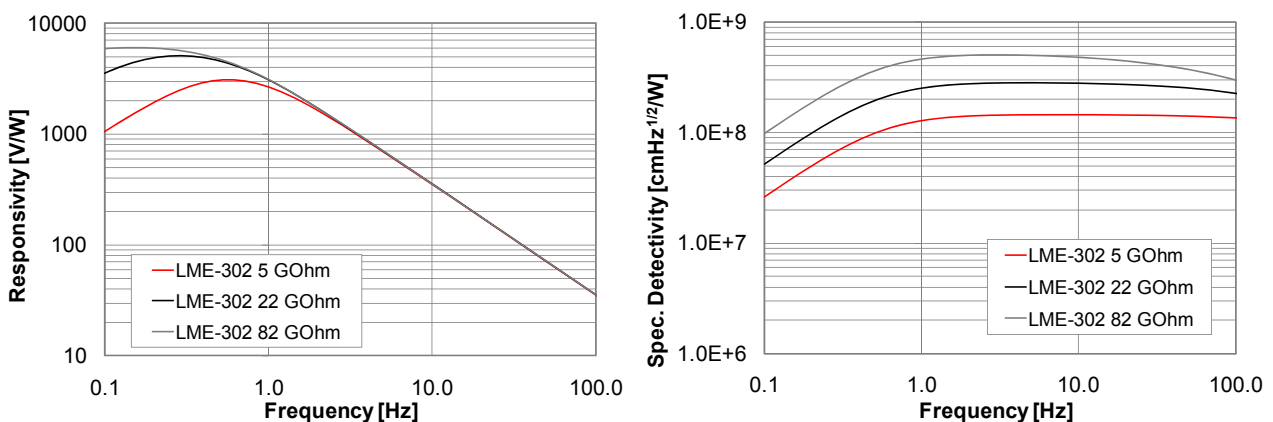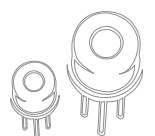
Fig 8: *Frequency response of responsivity (signal) and specific detectivity (signal-to-noise ratio) as a function of the gate resistor in voltage mode detectors; LME-302 (standard 82 GOhm, for comparison with 22 and 5 GOhm)*

Advanced Features

2 Microphonic Effect in Pyroelectric Detectors

2.1 Basics

All pyroelectric crystals are inherently piezoelectric. When a pyroelectric detector is mechanically excited through shock or vibration, an unwanted signal is produced. This behavior is called a microphonic effect or vibration response.

The interaction of mechanical and electrical variables in piezoelectric crystals can be expressed in an open-circuit operation by a simplified equation for the electrical field strength E and its dependence on stress T as shown in table 1. Depending on the orientation of the stress, two basic effects can be distinguished: the Transverse Effect (along the chip edges) and the Longitudinal Effect (through the thickness).
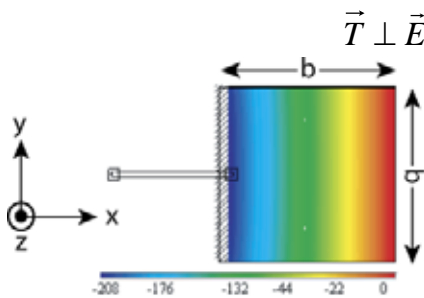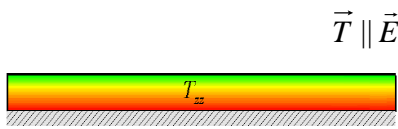
	Transversal Effect	Longitudinal Effect
	$\vec{T} \perp \vec{E}$	$\vec{T} \parallel \vec{E}$
Model		
Open-circuit voltage	$u_{vib} = -\dfrac{d_{31}}{\varepsilon_0 \varepsilon_{T33}} \dfrac{\rho b h}{2} \widetilde{a}$	$u_{vib} = -\dfrac{d_{33}}{\varepsilon_0 \varepsilon_{T33}} \dfrac{\rho h^2}{2} \widetilde{a}$
Open-circuit voltage of a 30 µm thick LiTaO$_3$ chip, 3 mm sq. element size, acceleration 9.81 m/s² (b=3 mm, h=30 µm, a=1 g)	$u_{vib} = 25\ \mu V$	$u_{vib} = 0.8\ \mu V$

Table 1: Comparison of transverse and longitudinal effect on a square thin chip

If the stress T is applied into the plane of the chip and transverse to the electric field strength E one can use the transversal model. The stress is a linear function in the X direction and exhibits its maximum value at the bearing point and zero-crossing at the right border. The mean stress is half of the maximum stress T_{XX}. A lithium tantalate element with a square electrode of (3 x 3) mm and thickness of 30 µm would produce an open-circuit vibration voltage of about 25 µV at 1 g (9.81 m/s²). If the acceleration acts longitudinal to the electrical field strength E and out of the plane of the chip the open-circuit vibration voltage per g is about 0.8 µV for a 30 µm thick lithium tantalate chip. This vibration voltage represents a limit for the reduction of the microphonic effect for a single element. Any further reduction could be achieved only by adding an anti-parallel/anti-serial compensating element.
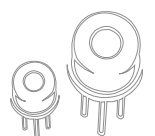
Advanced Features

2.2 Reduced microphonic voltage by 'in-chip-compensation'

The simplest solution for reducing the stress caused by the transverse effect is the simultaneous clamping of the chip, both at the left and right borders. This results in tensile and compressive stress in the halves of the element and would counterbalance each other. A central fastening leads also to the compensation of stress. As shown in figure 9 the open-circuit vibration voltages are minimized by both the fastenings.
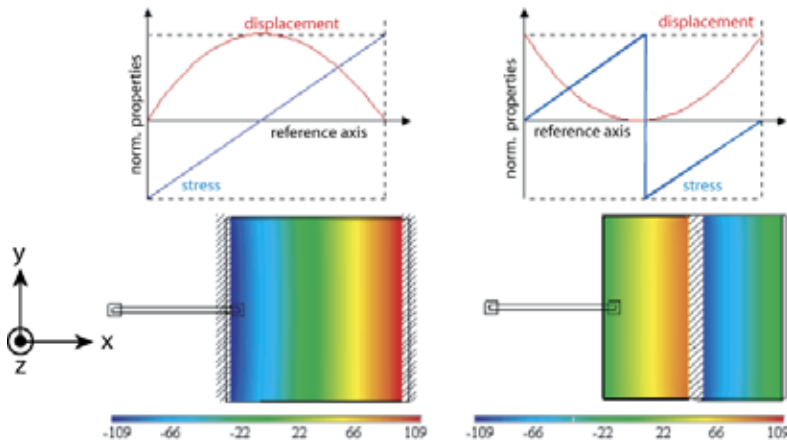

Fig 9: Stress distribution on a double-sided (left), and center (right) clamped pyroelectric detector chip (3 x 3 x 0.03) mm^3 with acceleration in the X direction

The analytical description of the microphonic effect shows that the transverse effects are minimized by an outer symmetrical mounting, or a central mounting and that the longitudinal effect is much lower. However, stress overshoot around the mounting points is produced, when the acceleration is applied out-of-plane. In this case the simplified analytical description of the longitudinal effect does not provide proper results, since the chip structure and chip mounting varies significantly from the ideal configuration. In contrast to the ideal configuration, the arrangement and thickness of the electrodes is different. Furthermore, an additional absorption layer displaces the neutral stress line out of the center line. The influence of an acceleration out-of-plane could only be described accurately by a numerical analysis, for example by the simulation software ANSYS Multiphysics.

As shown in figure 10, the base for the numerical analysis is a chip holder. The chip holder consists of a base plate with a central column surrounded by four symmetrically arranged columns. The pyroelectric chip is assembled on the chip holder by adhesive bonding.
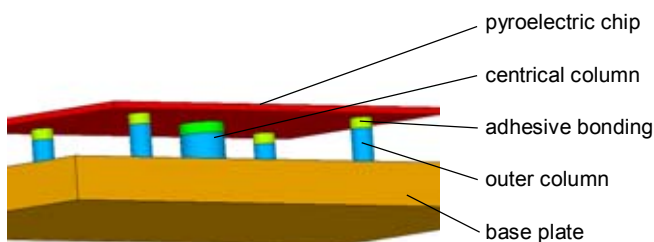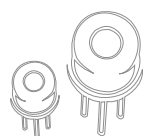

Fig 10: Model of the assembly of chip holder and pyroelectric chip

Advanced Features

In the plane of the pyroelectric chip the open-circuit vibration voltage is compensated by the symmetrical arrangement of all columns. If we look at the out-of-chip plane, the open-circuit vibration voltage is compensated by the arrangement of the outer surrounding columns in such a manner that convex and concave warpings are induced by mechanical excitation in the normal direction. These warpings produce tensile and compressive stress at one surface and the reversed at the opposite side of the pyroelectric chip as illustrated in figure 11. The positive and negative piezoelectric charges generated by the stress are compensated by the electrodes, which cover the top and the bottom sides. To achieve a stress compensation, the chip deformation can be optimized by modifying the arrangements of the mountings (see figure 12).
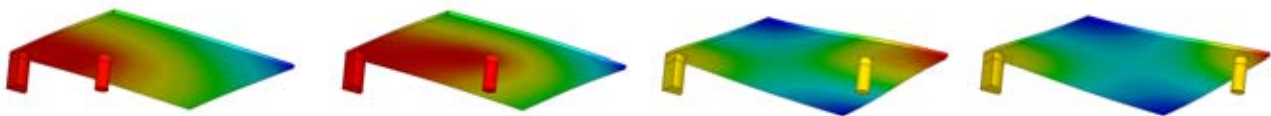

Fig 11: Deformation and stress of a quarter of a pyroelectric chip assembled on a chip holder using different support positions along the chip diagonal
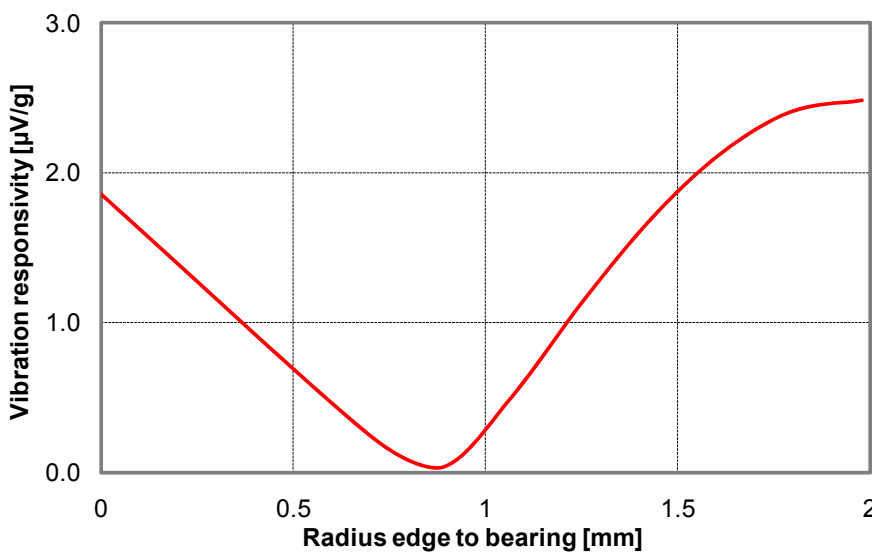

Fig 12: Acceleration response of the chip shown in figure 11 as a function of the mounting point position

The stress distribution inside of a pyroelectric chip is also affected by the chip coating, technological parameters, as well as the elastic modulus of the adhesive by which the pyroelectric chip is bonded onto the chip holder. Nevertheless, the statistics of sample measurements confirmed a good fitting of the test results and simulated values.
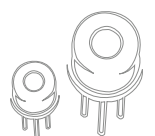
Advanced Features

2.3 Microphonic effect at Voltage and Current mode operation

The operational mode of a pyroelectric detector and the frequency range affects the result of piezoelectricity at detector's output (see figure 13).

Voltage mode

The Open-circuit operation of a pyroelectric chip as described in the earlier 'Detector Basics' section is given typically in voltage mode for frequencies higher than 0.5 Hz. The criteria for this is the electrical break point set by the product of chip capacity C_P (30 ... 120) pF and gate resistor R_G (5 ... 100) GOhm. In this frequency range the vibration or so called microphonic voltage at the detector output is identical with the open-circuit vibration voltage (see 'Detector Basics'):

$$u'_{vib\,VM} = u_{vib} \tag{1}$$

A typical signal of a voltage mode detector is in the order of millivolts. A 100 g acceleration (e.g. a shock) can produce a similar but disturbing signal of the mechanical vibration if its frequency fits the amplifier pass band.
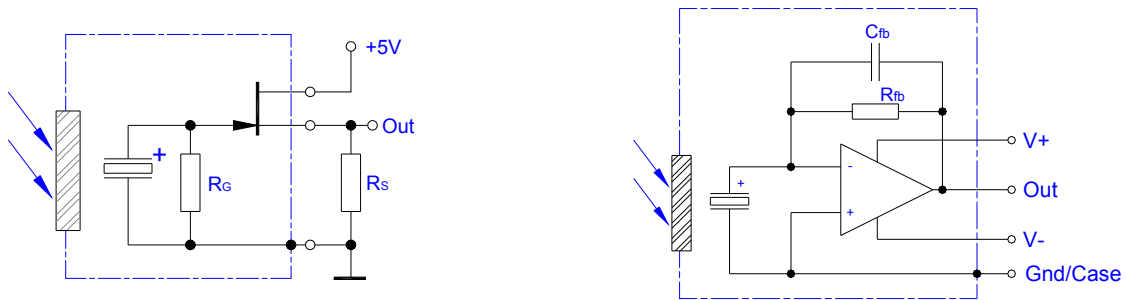

Fig 13: Voltage mode operation (left) and current mode operation (right) of a pyroelectric detector

Current mode

State-of-the-art pyroelectric detectors make more and more use of the current mode (see figure 13). From the open-circuit vibration voltage u_{vib} the short-circuit current i_{vib} is derived, which increases in a linear manner with the frequency. The short-circuit current flows in a preamplifier and generates a signal voltage u' at the output:

$$u'_{vibCM} = i_{vib} \cdot R_{fb} \frac{1}{\left[1+(\omega\tau_E)^2\right]^{1/2}} \tag{2}$$

As in voltage mode operation the microphonic voltage at detector's output is constant for frequencies well above the electrical cut-off frequency. Because the electrical time constant in current mode is defined by the feed back components C_{fb} and R_{fb} (this time constant is clearly shorter) this frequency range starts only from some 10 Hz. In this frequency range the vibration voltage at the detector output is created by the open-circuit
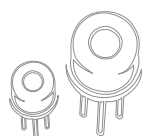
Advanced Features

vibration voltage but amplified by the quotient of the capacitance of the pyroelectric chip and of the feedback capacitance:

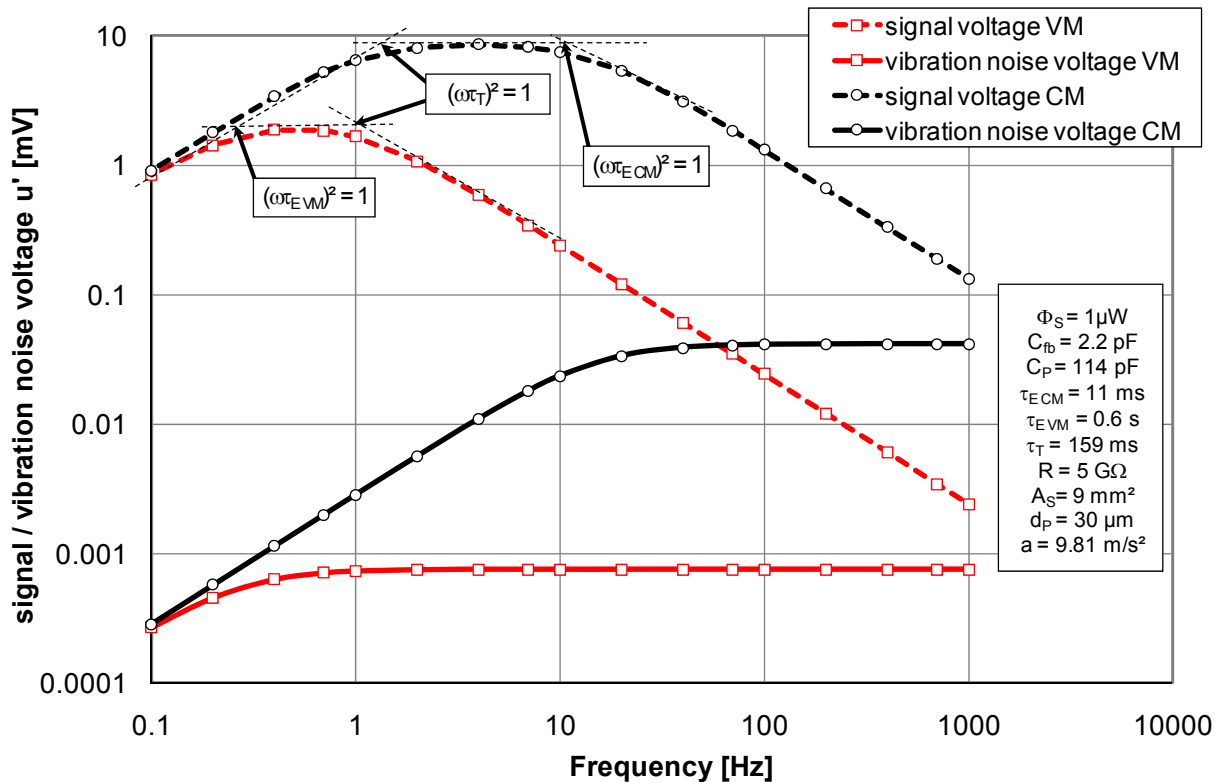$$u'_{vib\,CM} = u_{vib} C_P C_{fb}^{-1} \tag{3}$$

Comparison

Fig 14: *Comparison of the signal voltage u'$_S$ and of the vibration interference voltage u'$_{vib\,z}$ (longitudinal effect) in voltage mode and current mode*

Figure 14 shows the frequency correlations with straight lines for the vibration voltage and dashed lines for signal voltage. The results are indicated with circles and squares for the current mode and the voltage mode respectively. Even if the vibration voltage behaves differently for current and voltage mode the ratio of signal to vibration voltage at a specific frequency (means the distance between the two red or the two blue lines in the diagram) is the same for current and voltage mode. There is no advantage from point of vibration responsivity by using current or voltage mode.
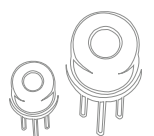
Advanced Features

2.4 Introduction of the term 'Microphonic-Equivalent Power (MEP)'

InfraTec introduced the Microphonic-Equivalent Power (MEP) for a simplified discussion:

$$MEP = \frac{R_{vib}}{R_V} \tag{4}$$

with

$$R_{vib} = \frac{u'_{vib}}{\tilde{a}} \tag{5}$$

The MEP is defined as the quotient of the vibration responsivity and voltage responsivity and indicates the incident radiation flux, required to generate an equivalent root-mean-square (rms) signal voltage for a given vibration. It is expressed in the units of W/g (*gravitational acceleration g = 9.81 m/s²*). Table 2 summarizes vibration responsivity, voltage responsivity and MEP. Of course the MEP is more or less independent from the operation mode of the preamplifier. In the case of a standard detector, the vibration responsivity and hence the MEP strongly depend on the spatial direction of the applied vibration. In the case of microphonic reduced detectors ('low micro' type) with the novel chip holder, it is clearly demonstrated that the MEP value can be reduced to about (3 … 2) nW/g @ 10 Hz in all three spatial directions.

Detector	Vibration Responsivity R_{vib} (10 Hz, 25 °C) in µV/g			Voltage Responsivity R_v (500 K, 10 Hz, 25 °C) in V/W without window	Microphonic Equivalent Power MEP (10 Hz, 25 °C) in nW/g		
	x	y	z		x	y	z
LIE-502 (VM)	16	1,6	3,5	160	100	10	22
LIE-500 (CM)	550	55	120	5.500	100	100	22
LME-502 (VM)	0,5	0,5	0,4	160	3	3	2
LME-500 (CM)	65	65	50	22.000	3	3	2

Table 2: Vibration responsivity, voltage responsivity and microphonic-equivalent power of standard and 'low micro' detectors

Conclusion

There are four ways to reduce the influence of the piezoelectric behavior on pyroelectric detectors in customer's sensor modules:

- Suppress mechanical vibrations as much as possible by pulse damper (smooth rubber, flexible cables). Please note that the elongation [mm] at a constant acceleration [m/s²] is frequency dependent. A sinusoidal acceleration of 1 g = 9.81 m/s² is the result of a peak-to-peak elongation of:

70 cm at 1 Hz	7 mm at 10 Hz	70 µm at 100 Hz	0.7 µm at 1 kHz

- In a compact sensor module mechanical damping can only be realized for frequencies higher than 100 Hz.
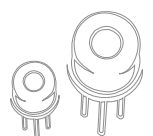
Advanced Features

- Limit the electrical pass band of the amplifier stages especially at the high frequency side by a steep low pass.
- Compensation of the microphonic voltage by sophisticated mounting of the pyroelectric chip.

InfraTec offers a variety of pyroelectric detectors in voltage mode (VM) or current mode (CM) operation with a reduced vibration response (so called 'low micro') based on InfraTec's patented chip mounting technology. The reduction of the microphonic voltage is in the order of a twentieth (5 %) of a conventional pyroelectric detector. Figure 15 shows their typical frequency response. Please note that the differing vibration voltage of the CMOS OpAmp detector series LME-351, -341 and -335 caused on a differing gain. LME-335 offers the highest responsivity (90,000 V/W @ 10 Hz).
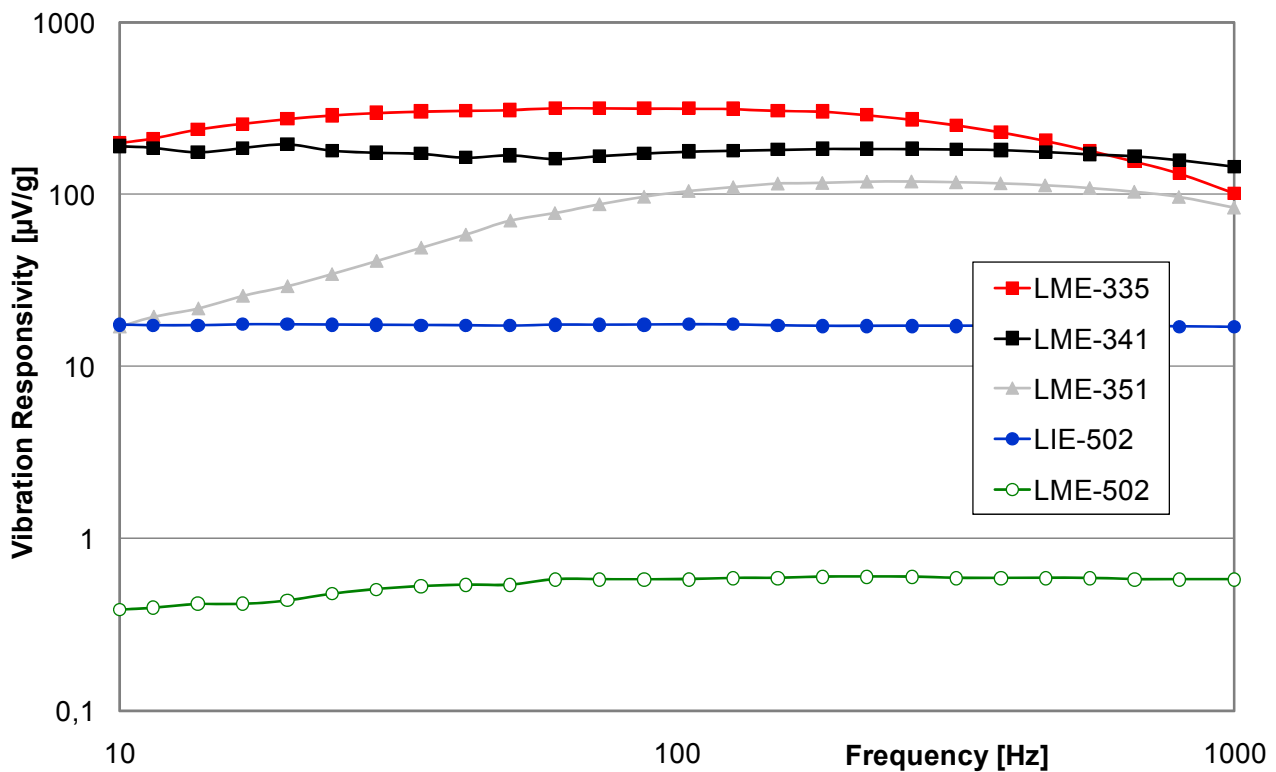

Fig 15: Test results of microphonic effect
LME-502 (VM, (3 x 3) mm^2, 'low micro'), LIE-502 (VM, (3 x 3) mm^2, conventional),
LME-351 (CM, (2 x 2) mm^2, 'low micro', 5 GΩ // 0.2 pF), LME-341 (CM, (2 x 2) mm^2, 'low micro',
24 GΩ // 0.2 pF),

InfraTec's 'low micro' technology is available for single element detectors such as LME-316 (VM) or LME-345 (CM) and multi color detectors such as LMM-244 with an element size of (2 x 2) or (3 x 3) mm². These detectors can be identified at the part description by an 'M' in the second digit (LME instead of LIE or LMM instead of LIM).
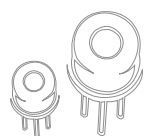
Advanced Features

3   Beamsplitter Detectors – Even for the narrowest signal beams

The construction of multi color detectors with integrated beamsplitter is shown in the following picture. The IR radiation entering through the aperture is divided by a beamsplitter in two or four parts (4 channel pictured). Each of the partial beams goes through an IR filter and finally hits a pyroelectric detector chip. This design works well with single narrow-beam sources or in situations where contamination (dust, insects) in the light path could be an issue.
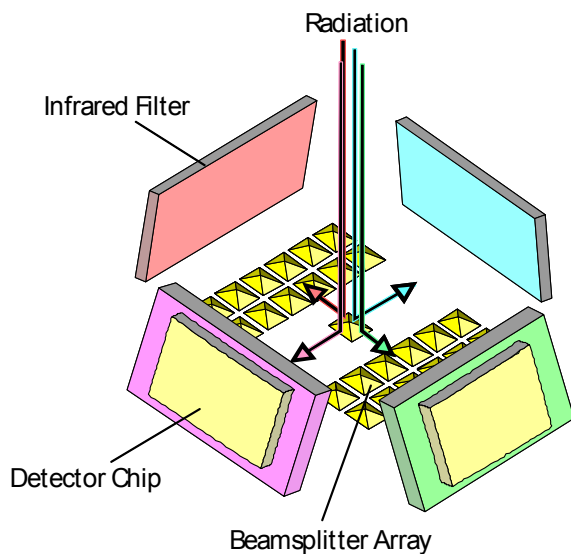

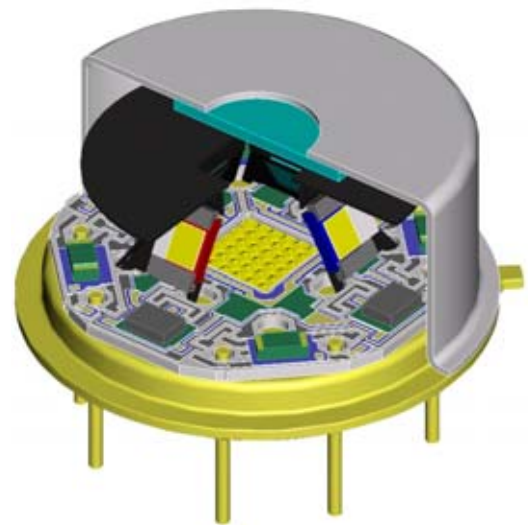*Fig 16: Principle of reflective beamsplittering*   *Fig 17: 3-D Design LIM-054*

3.1   General design

The beamsplitters are made of gold plated microstructures for the two and four channel devices to achieve a homogeneous distribution of the radiance. The filters are mounted at a certain angle to obtain a normal incidence of the radiation. This configuration avoids drifts in the filter transmission curves to shorter wavelengths and the influence of the opposite filter (reflections).

In addition to four channel beamsplitter detectors using four-sided micro pyramids, InfraTec has also developed two channel detectors based on micro V-grooves. In the following figure SEM images of two and four channel beamsplitters are shown. The V-groves pitch is 100 μm and the pyramids are 50 μm, with the tilt angle of the filters and detectors set at 30°.
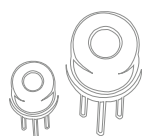
Advanced Features

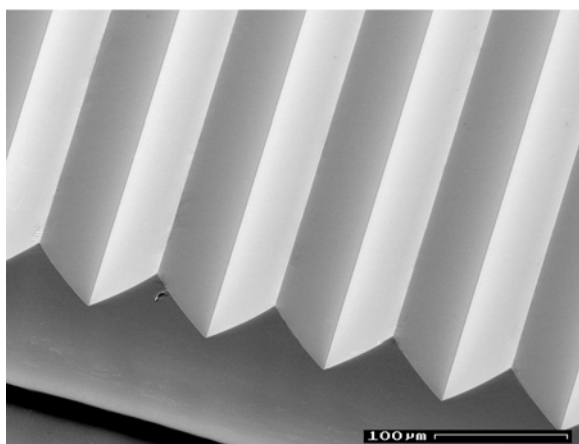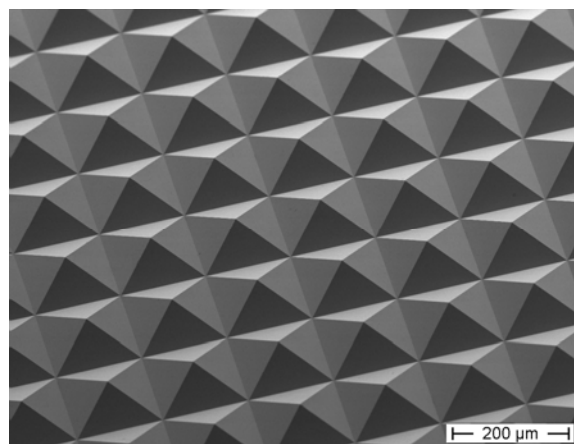

Fig 18: Micro groove (2-channel)

Fig 19: Micro pyramids (4-channel)

3.2   Comparison to other multi channel detectors

The beamsplitter detector has a single aperture compared to conventional multi channel detectors**.** It is possible to use a gas cell with a smaller diameter reducing the gas volume. A smaller gas volume reduces the size of the sensor module and accelerates the gas exchange. Also, the signal ratio of all channels is independent from aging, mechanical shift or pollution processes among one another.

The **multi color** detectors should be used for the analysis of gas mixtures with few known gases. Typical examples for a successful application are anesthetic gas monitors and the pulmonary function testing. **Variable color** detectors as described in the following allow a more flexible operation of the analyzer enabling the detection of adjoining or overlapping absorption bands. So far the measurement of single gases like ethanol and carbon dioxide as well as gas mixtures of methane, propane and anesthetic gases have been tested. In the following table characteristics of the multi and variable color detectors are summarized.

Detector Specification	Multi Color	Multi Color	Variable Color
Principal	Individual Windows	Beamsplitter	Tunable Fabry-Pérot Filter
Filtering	Parallel	Parallel	Serial
Area to be illuminated	Ø 9.5 mm	Ø 2.5 mm	Ø 1.9 mm
Spectral Range	(2 … 25) µm	(2 … 25) µm	(3.0 … 4.1) µm (3.9 … 4.8) µm (8.0 … 10.1) µm
Current Mode (available)	Yes	Yes	Yes
Voltage Mode (available)	Yes	Yes	No
Thermal Compensation	Yes	No	Yes
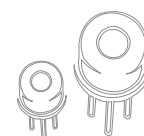
Advanced Features

4 Basics and Application of Variable Color Products

The key element of InfraTec's variable color products is a silicon micro machined tunable narrow bandpass filter, which is fully integrated inside the detector housing. Applying a control voltage to the filter allows it to freely select the wavelength within a certain spectral range or to sequentially measure a continuous spectrum. This design is very different from detectors with fixed filter characteristics and enables the customer to realize a low resolving and low cost spectrometer. The variable color product group currently includes the

- LFP-3041L-337
- LFP-3950L-337
- LFP-80105-337

which differ in the wavelength range they each cover. The pyroelectric detector used is similar to the standard **LME-335** device, but with a shorter electrical time constant. New types and wavelength ranges may be introduced in the future.

4.1 Fabry-Pérot filter (FPF)

The tunable filter is based on the well-known Fabry-Pérot Interferometer (FPI). Two flat and partially transmitting mirrors, characterized by reflectance **R** and absorptance **A,** are arranged in parallel at a distance **d**, forming an optical resonator with the refractive index **n** (figure 20 left).

The beam with intensity **I₀,** incident under the angle **β**, is reflected back and forth inside the resonator. Multiple-beam interference generates a pattern of successive peaks in the transmittance spectrum **T(λ)** of the FPF (figure 20 right), described by the Airy formula
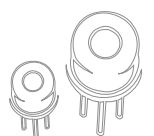
$$T(\lambda) = \frac{I_t}{I_0} = \frac{T_{\max}}{1 + F \sin^2\left(\dfrac{2\pi n\, d \cos \beta}{\lambda}\right)} \tag{6}$$

with the peak transmittance

$$T_{\max} = \left(1 - \frac{A}{1-R}\right)^2 \tag{7}$$

and the finesse factor

$$F = \frac{4R}{(1-R)^2} \tag{8}$$
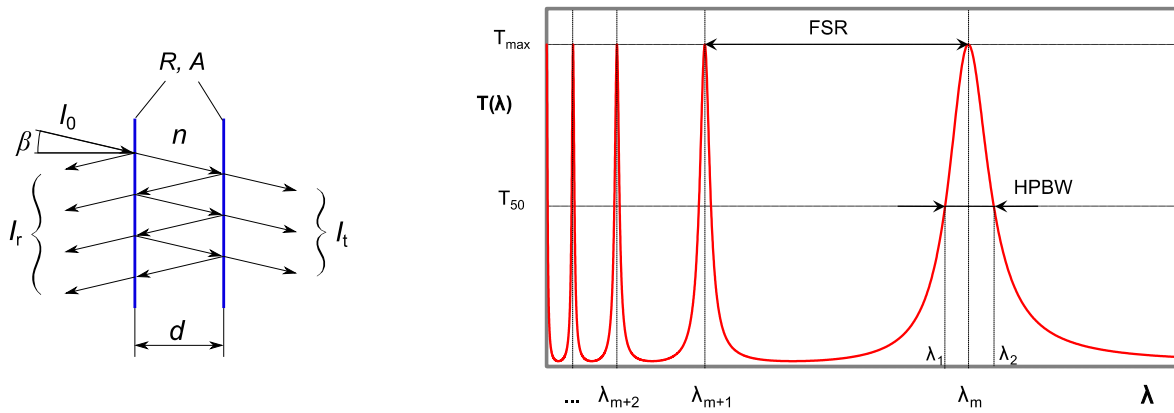
Advanced Features

Fig 20: Schematic configuration and transmittance function of the Fabry-Pérot Interferometer

The transmittance peaks of different interference orders **m** are located at wavelengths, for which the resonance condition

$$\lambda_m = \frac{2\,n\,d\,\cos\beta}{m} \tag{9}$$

is met. The FPI can be used as a tunable narrowband filter, if the desired order is selected by means of an additional broad bandpass filter (order sorting filter, blocking filter) and if the resonator gap **d** can be adjusted to tune the transmitted wavelength **λ_m** within the given free spectral range **FSR** for this order. The characteristic filter parameters of an FPF can be derived from the previous equations. In all types, that are currently available from InfraTec, the first interference order is used (**m = 1**). Given that **n = 1** (air inside the gap) and **β = 0** (normal incidence), the equations can be further simplified. The center wavelength **CWL** is defined as the mean value of the two half-power-points (**T_{50}**) in terms of wavenumbers:

$$CWL = \frac{2\lambda_1\lambda_2}{\lambda_1 + \lambda_2} \tag{10}$$

(Because of the periodicity of the Airy formula (eq. 6) in wavenumbers, calculation of the **CWL** in the wavenumber domain is preferred over wavelengths. In general, calculation of the **CWL** of interference filters in the wavenumber or wavelength domain are both common). The half-power bandwidth **HPBW** is the decisive factor for the spectral resolution:

$$HPBW = 2d\,\frac{1-R}{\pi\sqrt{R}} \tag{11}$$

The ratio of **FSR** and **HPBW** (calculated in terms of wavenumbers) is called the finesse $\tilde{F}$. In the theoretical ideal case (perfectly flat, smooth and parallel mirrors, collimated beam) it depends only on the reflectance **R** (reflectance finesse $\tilde{F}_R$)

$$\widetilde{F}_R = \frac{FSR}{HPBW} = \frac{\pi\sqrt{R}}{1-R} = \frac{\pi\sqrt{F}}{2} \tag{12}$$

In practice the finesse is limited by imperfections of the mirrors and the angle distribution of the transmitted beam.
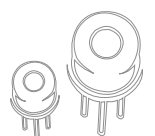
Advanced Features

4.2 Variable Color detector

InfraTec's FP filters are fabricated with silicon bulk micromachining technology and wafer bonding. Bragg reflectors for the specific wavelength ranges are coated on thick silicon carriers to guarantee a high finesse. The back sides are anti-reflection coated. The fixed bottom carrier is equipped with control electrodes, whereas the upper reflector is suspended by springs (figure 21). Applying a voltage V_c to the electrodes creates an electrostatic force, which decreases the resonator gap d and, consequently, tunes the filter wavelength.
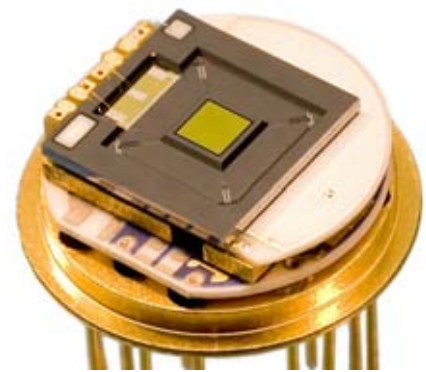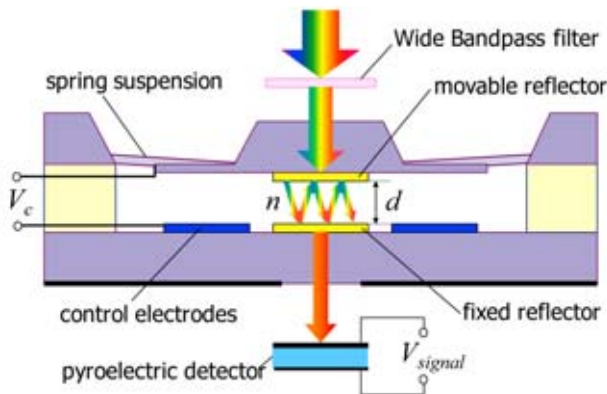

Fig 21: Schematic configuration (left) and picture (right) of the variable color detector

The MOEMS FPF is integrated in a TO8 housing together with a pyroelectric detector (figure 21). The latter is a state of the art thermally compensated current-mode type, similar to LME-335 but with smaller feedback capacitance. This results in a flat frequency response up to several tens of Hz. The thermal time constant is in the range of 150 ms. The element size of (2 x 2) mm^2 matches the size of the filter aperture (Ø 1.9 mm). The broad band pass blocking filter is integrated in the cap.

The mirrors of the FPI are made from dielectric layer stacks (Bragg reflectors) with a limited width of the reflective band (stop band). Therefore, the usable tuning range in the first order is less than expected from the theoretical **FSR**. Besides this, the reflectance and, consequently, the finesse vary over the tuning range ($\tilde{F}_R \approx 40\dots80$)**.** Tuning the **CWL** therefore results in a variation of the **HPBW** and the peak transmittance within certain limits. Figure 22 shows the typical variation of the **HPBW** and the limits given by fabrication tolerances. **HPBW$_{min}$** corresponds to the center and **HPBW$_{max}$** to the upper end of the tuning range.
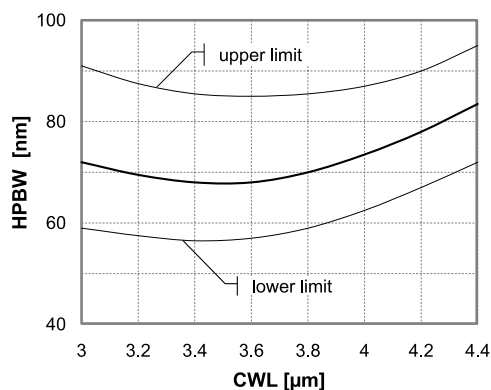
Filter code	HPBW$_{min}$	HPBW$_{max}$	Tolerance range
3041L	68 nm	85 nm	+85 … 95 nm -55 … 70 nm
3950L	75 nm	93 nm	+90 … 110 nm -65 … 80 nm
80105	130 nm	220 nm	+170 … 270 nm -100 … 180 nm

*Fig 22: HPBW over tuning range, typical values and tolerance range. **left:** curves for LFP-3041L-337;*
*   **right:** table for the currently existing filter types (measured with FTIR, ±6°, 4 cm^{-1})*
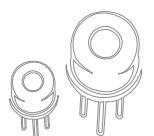
Advanced Features

The broad band pass and the pyroelectric detector element also show some spectral characteristics. The spectral response of the detector is a superposition of different fractions, but has to be considered as a whole in the application. At InfraTec, calibration measurements (figure 23) are performed by means of an FTIR spectrometer. The spectra are referenced to a 'black' detector with a flat spectral response and normalized to the highest peak (relative spectral response).
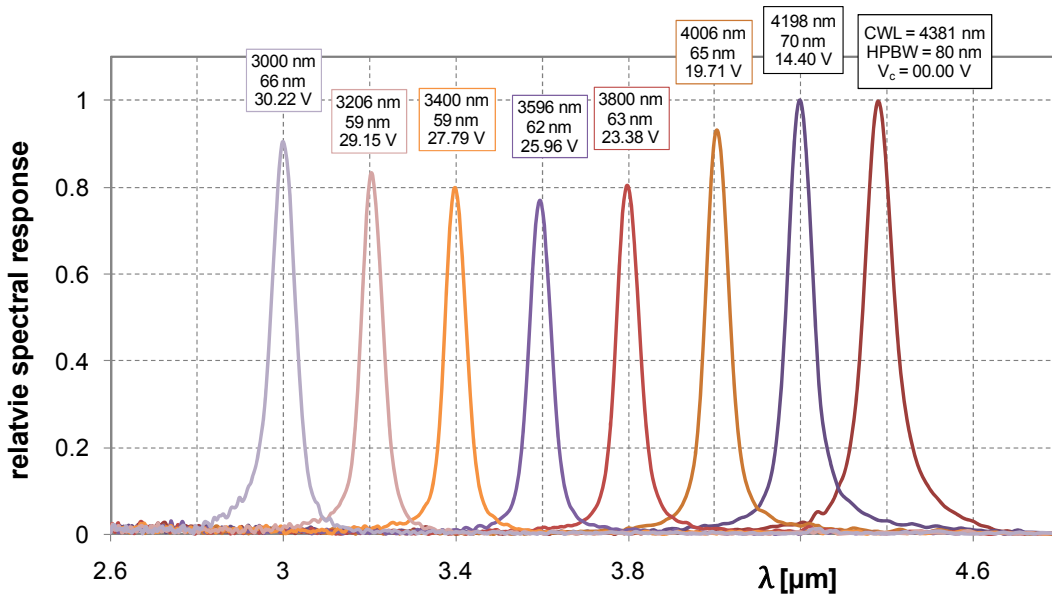

Fig 23: Relative spectral response of a FPF detector LFP-3041L-337 at several tuning voltages

4.3 Optical Considerations

The basic theory described in section 4.1 is restricted to simplified conditions, which requires a normal incident and perfectly collimated beam. An inclined but collimated beam results in a negative drift of the CWL (figure 24 left), but the most common case is an uncollimated beam with a certain angle of divergence and intensity profile. The resulting transmittance spectrum can be seen as the superposition of collimated raybeams with different angles of incidence and intensities. The superimposed spectrum has a broader HPBW and the CWL at slightly lower wavelengths (figure 24 right).
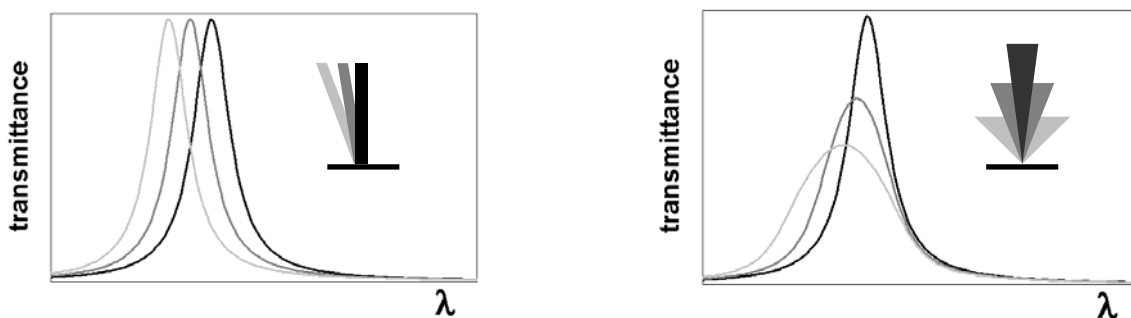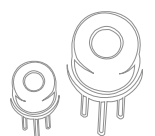

Fig 24: Influence of angle shift and divergence angle on bandwidth and peak transmittance of a FPF

Advanced Features

This effect is very well known from fixed interference filters but much more pronounced for FPF with a tunable air gap. Figures 25 and 26 show theoretical and measured values of the angle shift, relative to the ideal case (collimated).
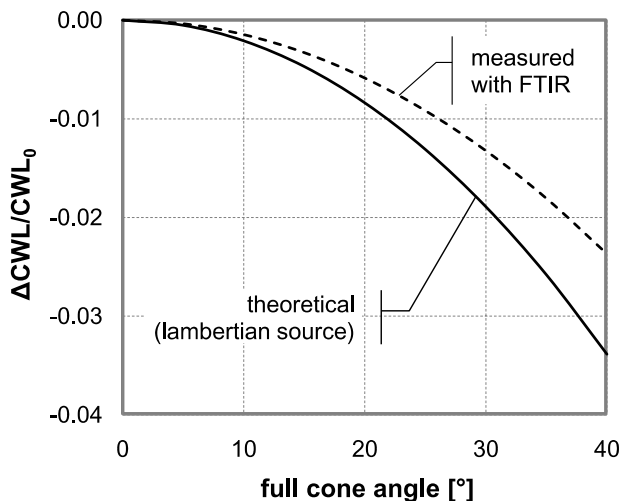

Fig 25: Relative shift of the CWL over the full cone angle, theoretical and measured with FTIR (mean angle of incidence 0°)
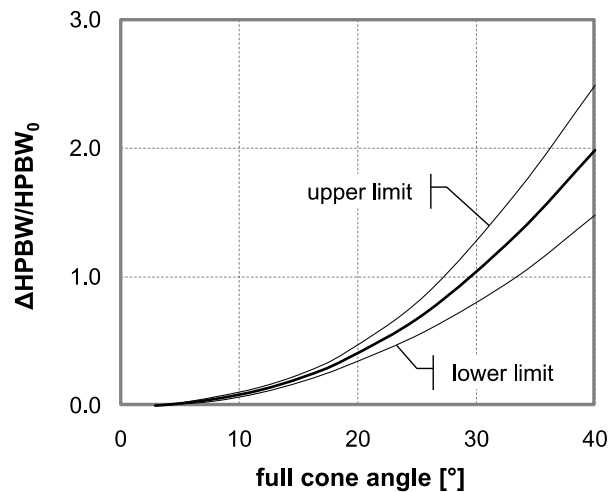

Fig 26: Relative shift of the HPBW over the full cone angle, measured with FTIR (mean angle of incidence 0°)

Wavelength shift depends only on the intensity distribution within the cone angle but not on the finesse. The thick curve (figure 25) may be considered as the worst case: a source with a lambertian intensity distribution. In practice higher angles often carry less intensity, which seems to be case in the FTIR measurement shown through the dashed curve. In contrast to the wavelength shift, the broadening effect depends on intensity distribution and the finesse (reflectance and surface defects of the mirrors). A higher finesse results in a stronger broadening (figure 26 upper limit) and vice versa. In the discussion above, normal incidence was considered. It is important to note, that illumination with an oblique (mean) <u>and</u> convergent (or divergent) ray bundle shift effects become even stronger and the spectra may be distorted dramatically.

Angle shift results in very important conclusions for the design and operation of FPF based analyzers or microspectrometers:

- The spectral performance of an instrument strongly depends on the optical conditions. As a consequence, the calibration of an FPF based instrument (wavelength and resolution) should be carried out within the final optical setup.
- For each particular application a compromise between spectral resolution and signal-to-noise ratio **SNR** (throughput) needs to be found. This is a principal rule, which is valid for all kinds of spectrometers.

Beam divergence can be minimized by using a light source with collimated output or by means of an additional prefixed aperture (figure 27 left). If the goal is to maximize the optical throughput, then focusing optics can be used, but larger cone angles will be a side effect (figure 27 right).
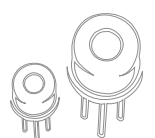
Advanced Features

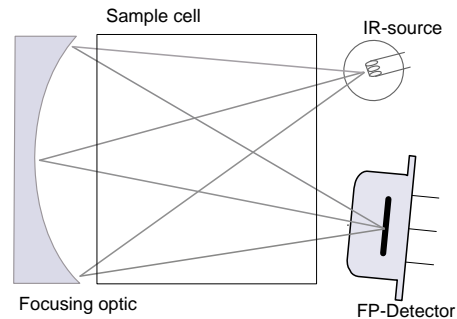**High Resolution**
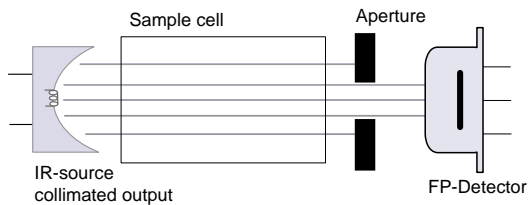
High SNR

Fig 27: Possible optimizations for the optical design of a microspectrometer with FPF detector
*   **left:** illumination with a parallel beam; **right:** illumination with a large cone angle*

Figure 28 shows the correlation of the achievable SNR with a given spectral resolution, measured with two tested measurement set ups according to figure 27. Please note that a parallel beam ø1 mm offers the highest spectral resolution but only 3 % of the intensity and thus the resulting low detector signal voltage compared to an illumination using f/1.4 optics.

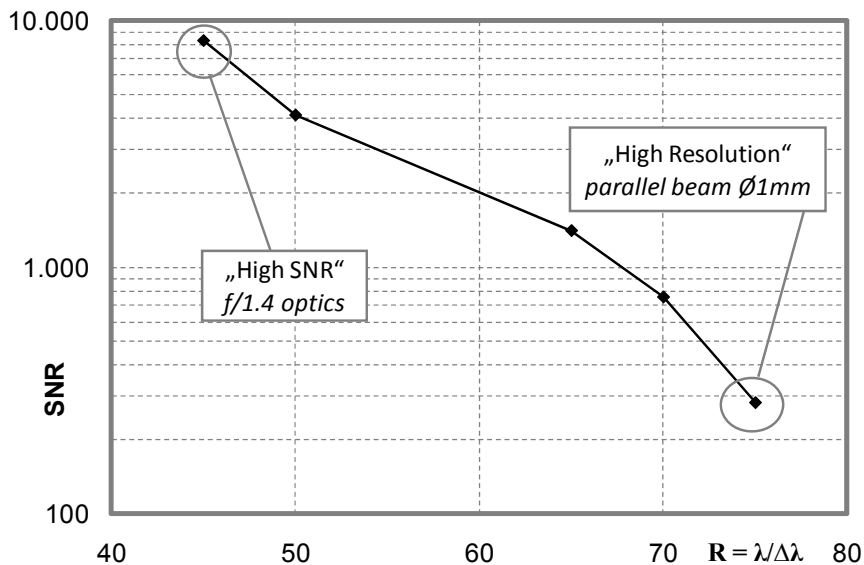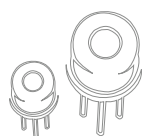*Fig 28: Measurements of the SNR vs. spectral resolution (LFP-3041L-337, modulated IR source at 10 Hz);*
*   **left end point:** Illumination with a large cone angle using f/1.4 optics **right end point:** Illumination with a parallel beam ø 1 mm*

Advanced Features

4.4 Filter operation

The filter is electrostatically driven. The control electrode (V_{c+}) is arranged at the fixed reflector carrier, while the movable reflector carrier acts as the counter electrode with the fixed reference potential V_{cref} (see figure 21). Applying a tuning voltage $V_c = V_{c+} - V_{cref}$ results in an electrostatic force F_{el} decreasing the electrode gap d_{el}.

$$F_{el} = \frac{\varepsilon_0 A_{el} V_c^2}{2 d_{el}^2}$$

(13)

As a first approximation the mechanical behavior of the FPI is that of an over-damped mass-spring system. Unfortunately, due to some nonlinearities like electrostatic softening and the squeeze film effect, damping ratio and effective stiffness of the system are functions of the actual mirror position and hence the filter wavelength. This behavior results – to give a first overview – in some practical constraints:

■ The filter is sensitive to acceleration forces: to vibrations (dynamic case) and to the position with respect to the earth's gravity as well (quasi static case).
■ Filter settling depends on wavelength.
■ The filter shows a stability limit at the so-called pull-in point. This should never be exceeded during operation, otherwise the filter could be damaged.
■ The filter wavelength can shift with temperature due to thermal expansion of the spacer layer.

Again it should be pointed out, that nearly all parameters, which describe the optical and mechanical behavior of the filter, depend on the mirror position and therefore on the filter wavelength. The points listed above are described in more detail in the following sections.

4.4.1 Electrostatic tuning

The quasi-static control characteristic is dominated by the quadratic dependence of the electrostatic force from the control voltage and the effective stiffness. Figure 29 shows a typical curve for the detector type LFP-3041L-337. Other filter types may differ in the voltage range but will exhibit the same behavior qualitatively.
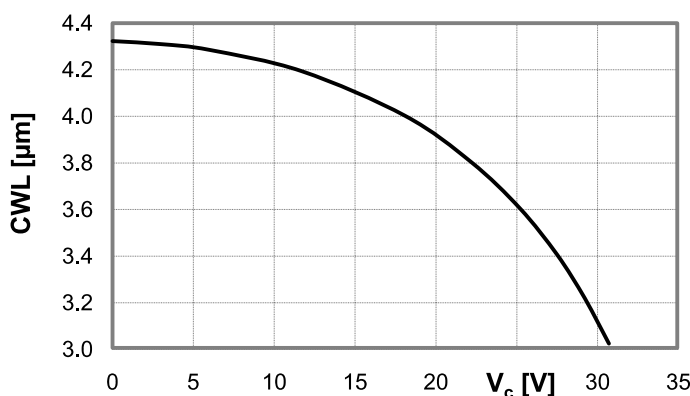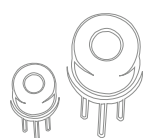

Fig 29: Typical steady-state control characteristic for LFP-3041L-337

Advanced Features

By analyzing equation (13) a positive feedback of d_{el} to the electrostatic force F_{el} becomes evident (electrostatic softening). The maximum stable operation range of a voltage controlled electrostatic actuator is therefore limited by the so called *pull-in* instability.

> The pull-in voltage should never be exceeded; otherwise the device may suffer irreparable damage. In practice this means: For each individual device (FPF) exists a maximum allowable control voltage for save and stable operation. Because of the fabrication tolerances, no general document like datasheets or application notes can provide this information to the user. One can obtain this from the individual measurement report only.

Furthermore, the polarity of the control voltage needs to be maintained, even as in equation (13) this does not seem to be necessary.

4.4.2 Dynamic behavior

■ The dynamic behavior of the filter can be approximated by a position dependent mechanical time constant τ (first order low pass), determined by stiffness and damping. For shorter wavelengths the system reacts slower, because the effective stiffness of the system is low and the air damping is high. Figure 30 gives typical values and the tolerance ranges, where τ_{min} corresponds to the upper and τ_{max} to the lower end of the tuning range.
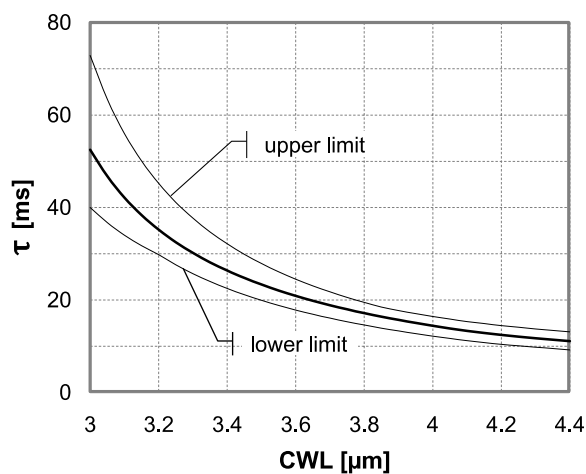

Filter code	τ_{min}	τ_{max}	Tolerance range
3041L	12 ms	55 ms	(±5…20) ms
3950L	10 ms	35 ms	(±5…20) ms
80105	3 ms	12 ms	(±1…4) ms

Fig 30: Time constant over wavelength, typical values and tolerance ranges;
left: curves for LFP-3041L-337; **right:** tabulated values for the currently existing filter types

4.4.3 Settling

When the filter is tuned from one wavelength to another by a control voltage step, it should be allowed to settle before the measurement is continued. The required settling time depends on the (absolute or relative) wavelength accuracy needed for the application and the step size. It can be calculated through the values given in figure 30. To give an example: The wavelength should be switched from 3.7 µm to 3.6 µm (type 3041L), the time constant in this region is about 20 ms. The settling time for the filter to stabilize within a tolerance of 5 nm of the final value (5 nm/100 nm = 5 %) is 3 * τ = 60 ms.
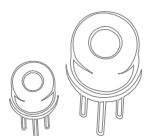
Advanced Features

Unfortunately, for the practical use of an FPF with a pyroelectric detector this is only part of the truth. Switching from one wavelength to another also causes a modulation of the radiation falling on the detector. In the worst case, a step over the entire tuning range, the detector 'sees' the complete spectrum (similar to the sweep mode, see section 4.5). Decisive for the settling of the detector output is the longest time constant in the system, which is the thermal time constant of the pyroelectric detector (in the range of 150 ms). How fast the 'measured value' settles, depends on the signal processing, too (bandwidth of software filtering, FFT/Lock-In). This subject is quite complicated and out of the scope of this application note.

4.4.4 Acceleration response

■   If the filter is exposed to acceleration forces, the upper reflector carrier will move and cause the filter wavelength to shift. The quasi-static response, like turning the filter with respect to the earth's gravity,   depends mainly on the effective stiffness and on the mass of the movable reflector. Figure 31 gives typical values and tolerance ranges, where CWL_{min} corresponds to the upper and CWL_{max} to the lower end of the tuning range.
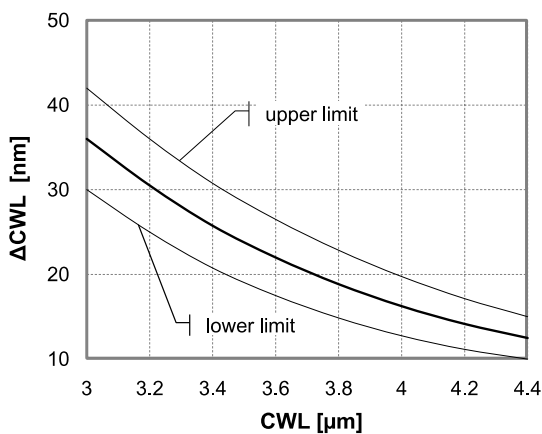
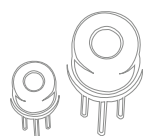| Filter code	ΔCWL_{min}	ΔCWL_{max}	Tolerance range
3041L	12.5 nm/g	36 nm/g	(±2.5…6) nm/g
3950L	12.5 nm/g	32 nm/g	(±2.5…5) nm/g
80105	25 nm/g	65 nm/g	(±7…25) nm/g

*Fig 31: Wavelength shift ΔCWL by gravity when turning the filter upside-down (± 1 g), typical values and tolerance ranges; **left:** curves for LFP-3041L-337; **right:** tabulated values for the currently existing filter types (1 g = 9.81 m/s²)*

In addition, the filter responds to dynamic vibrational forces, too. Due to the squeeze film effect, high frequency vibrations (see figure 30 for the mechanical time constants) are effectively damped.

4.4.5 Temperature shift

Interference filters are generally prone to a temperature shift, which is partly caused by purely mechanical expansion of the dielectric thin films and partly by a change of the optical constants of the materials. In case of tunable FP filters, the temperature shift is dominated by thermal expansion of the spacer layer, which defines the width of the air gap. As a temperature change mainly results in a mechanical detuning of the gap, the correlation between **HPBW** and **CWL** remains unchanged.

Again this effect is wavelength depended. At a given wavelength the temperature shift is nearly linear, and therefore a temperature coefficient TC_λ can be given. For shorter wavelengths the shift becomes larger, because of the reduced effective stiffness. Figure 32 gives typical values and tolerance ranges, where $TC_{\lambda min}$ corresponds to the upper and $TC_{\lambda max}$ to the lower end of the tuning range.

Advanced Features
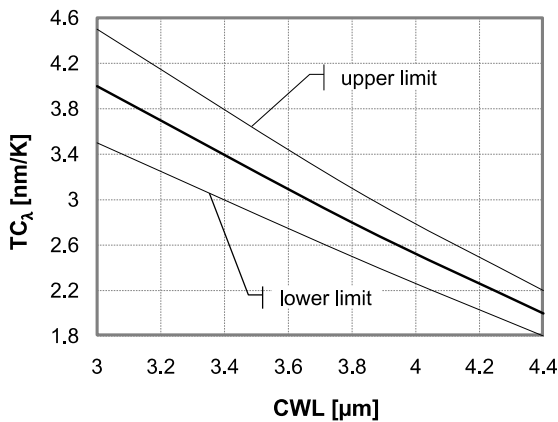
Filter code	$TC_{\lambda\,min}$	$TC_{\lambda\,max}$	Tolerance range
3041L	2.0 nm/K	4.0 nm/K	(±0.2…0.5) nm/K
3950L	2.0 nm/K	3.8 nm/K	(±0.2…0.5) nm/K
80105	2.0 nm/K	3.2 nm/K	(±0.5…1.0) nm/K

Fig 32: *Temperature coefficient of the CWL, typical values and tolerance ranges;*
left: curves for LFP-3041L-337; right: tabulated values for the currently existing filter types

4.4.6   Driving circuit

Figure 33 shows a suggestion of a driving circuit for variable color detectors. Gain and maximum control voltage should be selected according to the filter type. They can be adjusted through resistors R_2 and R_3.

The pins *Shield*, *Substrate* and V_{cref} should be on the same stabilized, low-impedance potential. Otherwise, spikes, ripples or other interfering signals at these circuit points or the control voltage as well may cause cross talk to the pyroelectric detector due to parasitic capacitances.

The combination C_5 and R_2 form a low pass filter, which helps to reduce voltage transients and therefore to reduce false signals. The time constant of any electrical filtering should be as high as possible, but should not exceed the mechanical time constant, so that the mechanical filter performance (settling) is not affected.
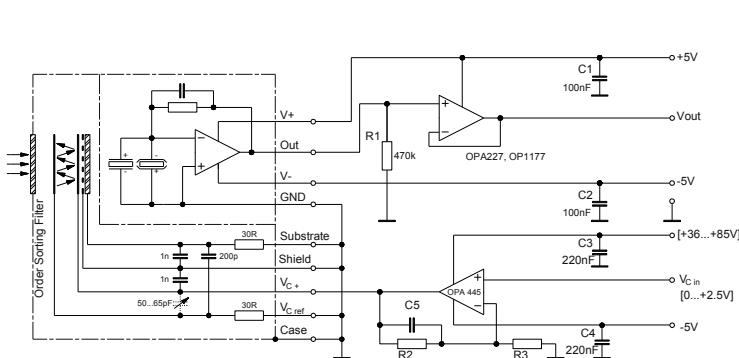

$$V_{c,max} = gain \times 2.5\,\mathrm{V} = \left(1 + \frac{R_2}{R_3}\right) \times 2.5\,\mathrm{V}$$

Filter code	$V_{c\,max}$	gain	R_2	R_3
3041L	33.8 V	13.5	150 kΩ	12 kΩ
3950L	69.5 V	27.8	150 kΩ	5.6 kΩ
80105	82.3 V	32.9	150 kΩ	4.7 kΩ

Fig 33: *Left: Recommended driving circuit for variable color detectors; right: dimensioning of the filter driving amplifier for several voltage ranges*

All data given in this note show the current stage of Fabry-Pérot product development. Our R&D team constantly works on further improvements which will be published in a suitable way such as updated data sheets.
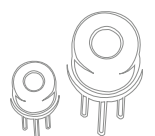
Advanced Features

4.5　Operation modes and measurement methods

The capabilities of variable color detectors are numerous. Depending on the measurement task and operation mode, different advantages compared to conventional single or multi channel detectors with fixed NBP filters can be found.

Hereafter three different operation modes will be explained in detail:

Sequence of channels

In the simplest case several fixed detector channels shall be substituted by a tunable detector. The filter is sequentially adjusted to the individual spectral channels. Besides the higher flexibility and expandability additional benefits may be given:

■　Simple multi channel detectors have separated apertures, which yield to the well known issues regarding non-uniform illumination, long-term stability, source drifting, pollution, etc. Tunable filter devices do not have these problems due to their principal design and singular light path.

■　Detectors with an internal beamsplitter also have a common aperture, but each channel is getting only a fraction of the whole radiant power. Applying the sequential measurement we can always use the whole incident radiant power. For four different channels and comparable conditions regarding aperture size and filter bandwidth theoretically a duplication of the SNR can be reached.

Step scan

The method described above can still be expanded in such a way that continuous spectra can be obtained. The required acquisition time for the mapping of a spectrum depends on the following facts:

■　Number of measuring points (wavelength range, step size):
　To get a continuous spectrum it must be scanned at minimum with a step size which corresponds to the half of the filter bandwidth (sampling theorem). Moderate oversampling can be useful, but will increase the measurement time.

■　Recordings of the measuring points (modulation frequency, integration time):
　These parameters define the SNR. Beside the detector properties and the applied analysis methods, the radiant power, modulation depth of the IR source and the design of the measuring section are crucial.

■　Settling time of the filter:
　The actual settling time of the filter depends on the wavelength as described earlier. It should therefore be implemented variably to achieve an optimum of speed.

As an example for measurements with the step-scan mode, figure 34 shows spectra of a polystyrene foil. The red squares are the 'steps' of the FPF (LFP-3041L-337), whereas the solid line is measured with an FTIR spectrometer for comparison.
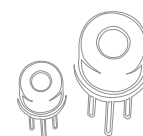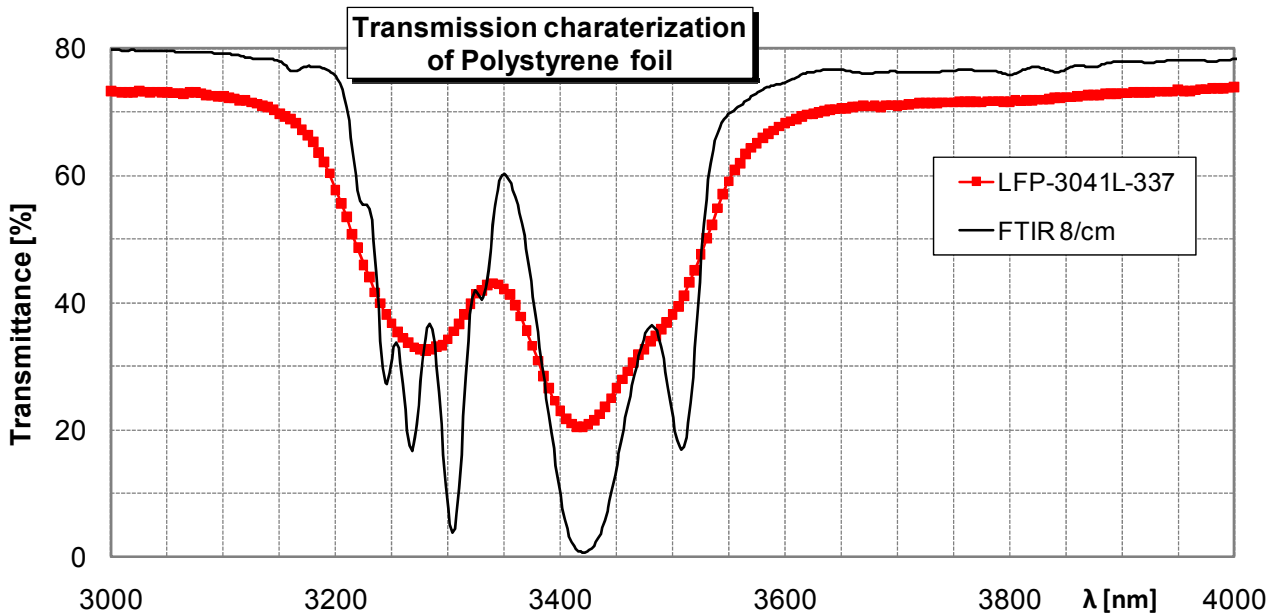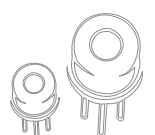
Advanced Features

Fig 34: Measurement example for the step scan mode (Polystyrene foil) LFP-3041L-337: spectral resolution R = 65; SNR ≈ 1,000:1; 100 data points; acquisition time 10 s

Continuous scan (Sweep mode)

By using a pyroelectric detector only modulated radiation can be analyzed. Normally this is realized by mechanical chopping or electrical modulation of the IR source. However, if the filter is continuously scanned (sweeped) the spectral information can be directly used for the modulation. The filter is actuated dynamically in this case.

This particular operation mode has principally the potential to accelerate the recordings of spectra remarkably. One possible application is the fast (presence) detection of films (e.g. a lubricant on a metal surface). Two basic approaches are possible for a dynamic operation:

- Presetting of voltage characteristics $V_c(t)$ for filter modulation (sinusoidal, ramp or similar…) and
    - Detection of the resulting function $CWL(t)$ by an adequate calibration scheme for example with wavelength standards (e. g. NBP filters) or
    - Evaluation of the detector signal with dedicated software algorithms (chemometric techniques)
- Presetting of a designated function $CWL(t)$ and determination of the appropriate voltage characteristic $V_c(t)$ for example with wavelength standards
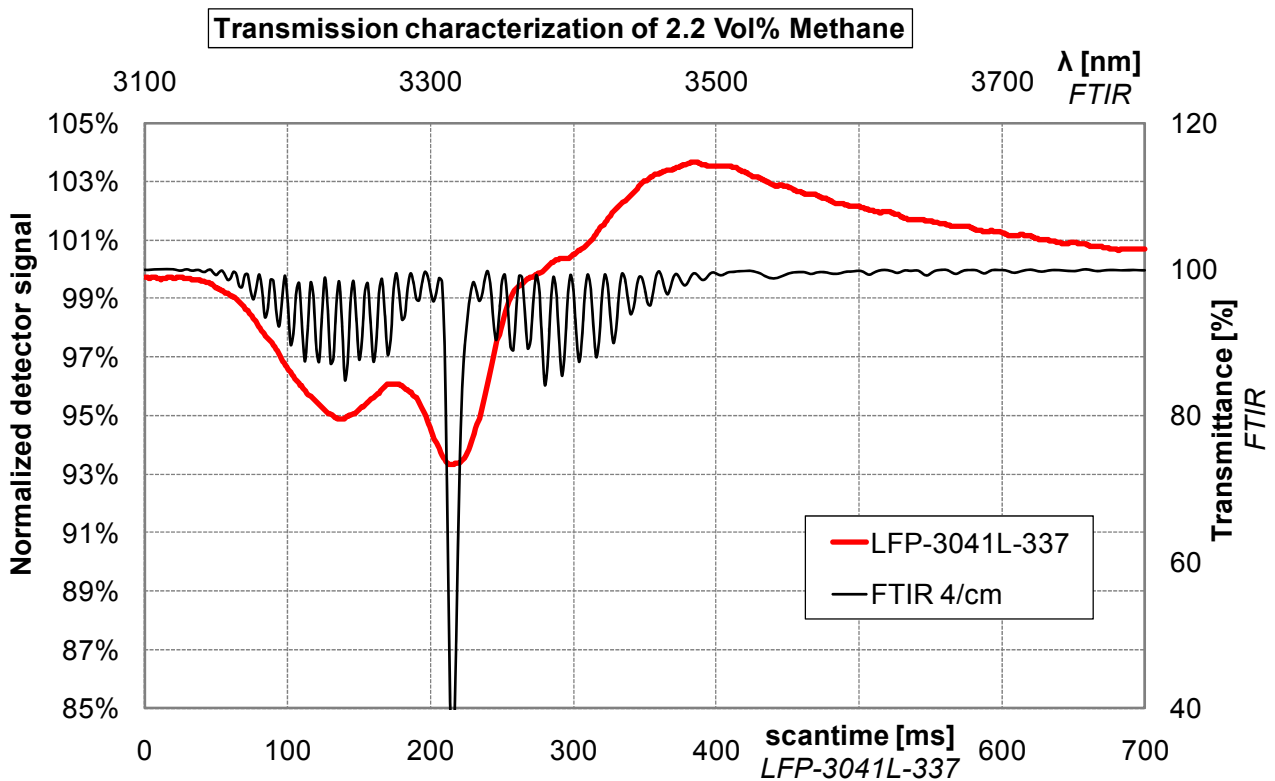
Advanced Features

Transmission characterization of 2.2 Vol% Methane

Fig 35:   Measurement example for the sweep mode with dynamic filter tuning (methane)

Figure 35 gives an example for the dynamic operation. The IR source is working in DC operation, while the filter goes through the desired wavelength range. Except for the DC-portion, the whole spectral information is contained in the generated detector signal. For the filter actuation and signal processing the dynamic properties of both, filter and detector, have to be considered.

4.6   Summary

With the extension of our product range by variable color detectors additional technologies are available for our customers. All types of our multispectral detectors are complementing one another:

- Conventional dual and quad channel detectors can be used in competitive volume applications
- Our dual and quad channel beamsplitter detectors with one aperture are used as long term stable and very accurate measuring modules for different spectral channels
- Variable color detectors with a high SNR allow a more flexible operation of the analyzer enabling for example the detection of adjoining or overlapping absorption bands. They are also of interest for applications, where more than 4 spectral channels shall be scanned within a short time frame.